International Research Journal of Engineering and Technology (IRJET) e-ISSN: 2395-0056
Volume: 06 Issue: 11 | Nov 2019 www.irjet.net p-ISSN: 2395-0072

Photovoltaic 10MW Power Plant Simulation & Design using Mathwork & Simulink Software

Miss. Sonawane K. D[1], Prof. Tapre P.C[2]

[1]*Maharashtra, India.*
[2]*Maharashtra, India.*

Abstract - *This study introduces modelling & simulating photovoltaic power generation system by using MATLAB & Simulink software. Now a days development in many sector depends on energy because energy is basic need of these sectors in the world. In available core energy sources such as oil, coal, gas, nuclear energy plants have limited resource & they have side effect on environment. Therefore renewable energy sources like solar, wind, marine energy are alternatives. Power plant is made by using photovoltaic panels & they arrange in parallel – series combination, 3-phase inverter(d-q theory with IP current regulator) connected to step up transformer (0.4KV low voltage grid and 20KV medium grid), DC-DC boost converter(MPPT controller). In many cases dynamic behavior of photovoltaic solar system are simulated. They gives solar irradiance and temperature changes.*

INTRODUCTION

The increasing number of renewable energy sources and distributed generators requires new ideas for the operation and management of the electricity grid in order to either maintain or even to increase capacity of the power-supply reliability and quality. The production of electrical vitality without polluting activities and on the environment and exhaustion of its resources is a very topical issue. The solar powered vitality radiation, considered relative to the life on Earth, seems to be limitless. The photovoltaic solar powered vitality relies on the direct generation of electricity by means of silicon cells. Under good climate conditions, when sparkling, the sun gives a power of 1 kW/m2. The photovoltaic board allow for direct transformation in electricity of 10…15% from the previously mentioned energy [1]. The efficiency of PV framework is a permanent concern [2]. The irradiance energy of the sun to electrical vitality can be converted through photovoltaic (PV) power age systems. If the power generation system does not exclude batteries to store the DC energy, rather including a common capacitor between the DC-DC and DC-AC converters to store the vitality on the side of DC-Link, then a fully non-contaminating source is obtained [3]. To get an advancement of the power supplied to the system, contingent on the irradiance intensity of the sun, it is preferred to choose a configuration in which the photo-voltaic power age system uses an efficient controller such as Maximum Power Point Tracking (MPPT) [4]-[11].

II) DESIGN OF THE PV POWER GENERATION SYSTEM

The outline of a PV power generation framework, with an installed power of 10 MW, is proposed in what takes offer. The electric power supplying by utilizing a PV equipment is made according to the pre-requirements imposed by the electric vitality provider who works at the PV site, two options being accessible: the low voltage connection (400 V) and the medium voltage association (20 kV), by means of the progression transformer (LV/MV).

The outlined PV power generation system is composed of (Fig.1

1) *A PV array* of PV panels combined in series and/or parallel strings such as to obtain a large power of 10 MW;

2) *A DC-DC boost* converter utilized as a load regulator and respectively to convert the yield voltage of the PV array to a suitable voltage for the inverter;

3) *A three-stage DC-AC converter* (i.e. inverter) to export the electrical energy to the three-stage grid;

4) *A three-phase* progression *transformer* to adapt the 0.4 kV low voltage output of the inverter to the 20 kV voltage of the grid;

5) *The PV power generation system controller*, which contains the MPPT controller for the DC-DC boost converter and the inverter's controller. The

Maximal Power Point Tracking (MPPT) is a technique impose to improve the effectiveness of power conversion in Photovoltaic (PV) systems. Under partially shadowed conditions, the Power-Voltage (P-V) characteristic exhibits multiple peaks and the available MPPT methods such as the Perturb and Observe (P&O) are incapable of searching for the Global Maximal Power Point (GMPP)

In Fig., *VOL* is the open-load voltage of the PV cell, *ISC* represents its short-circuit current value. *IMP* and *VMP* are the current and voltage associated to the maximum PowerPoint *PMP* .An algorithm was conceived and transposed in MATLAB, starting from the initial outline data.

1) Design of the PV array

Each panel (module) utilized by the designed establishment consists in cells of series connected polycrystalline cells. The front side of the PV module incorporates a highly straightforward glass sheet, characterized by a significant protection against mechanic stuns. The frame of anodized aluminum (covered through electrolysis by a layer of defensive oxide), shapes the structural help of the panel. All these give an adequate insurance against atmospheric agents like hail, snow, ice and storm. Every module contains by-pass diodes presented in the connection (dispersion) box. These diodes will permit the "off-lining" of the modules where the sunshine does not reach, in order to prevent their behavior as consumers for the modules getting radiation from sun and therefore restrict their undesired heat [3].

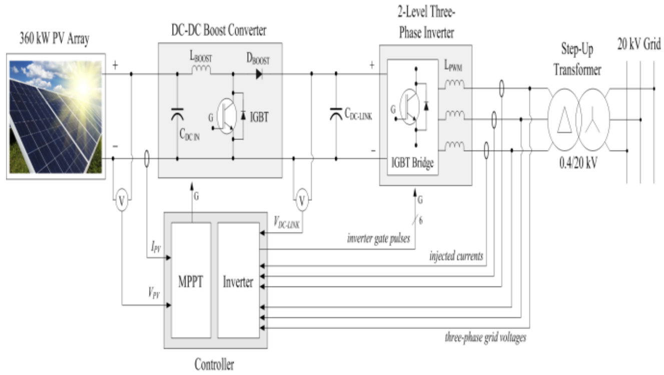

Fig. 1.The basic schematic of one 360 kW photovoltaic array generator.

Considering that the output voltage of a series arrangement PV modules is the sum of the component modules, and also considering the minimum DC-Link voltage for the inverter, one can got the number of PV modules arranged in series *NSER* based on:

$$N_{SER} = \frac{1}{2} \times \frac{(V_{DC-LINK})}{V_{MP}} \quad ...... \quad 1)$$

Where,

N_{SER} = number of necessary series connected modules;

$V_{DC-LINK}$ = the DC-Link voltage at the inverter input;

V_{MP} = PV module voltage at maximum power point;

A lower voltage can be selected for the inverter input, however as the voltage decreases (keeping the output voltage consistent), a higher current will flow through the DC-DC support converter. Therefore higher evaluated IGBT-s are needed. The minimum DC-Link voltage for the inverter can be registered with [3]:

$$V_{DC-LINK} \geq 2\sqrt{2} x V_{phase} \quad ...... \quad 2)$$

Where,

V_{phase} = the RMS value of the stage voltage at the inverter's yield.

Once the quantity of series connected modules is set, the quantity of strings in parallel is processed based on the appraised power of one inverter. One chose a 360 kW 2-level inverter offered by IGBT producer Semikron. The essential number of strings in parallel becomes:

$$N_{PAR} = \frac{P_{INV}}{P_{STRING}} = \frac{360\ kW}{2.47\ kW} = 146 \quad ...... \quad 3)$$

with: P_{INV} = the power of one inverter.

Thus, in order to calculate an installed power of 10 MW, we need a number of inverters N_{INV} and PV arrays N_{ARRAYS} given by:

$$N_{INV} = N_{ARRAYS} = \frac{P_{TOT\ MAX}}{P_{INV}} = \frac{10MW}{360KW} = 28 \quad 4)$$

with: $P_{TOT\ MAX}$ = required installed power for the PV park.

B. Sizing the DC-AC inverter

Inverter's sizing is finished considering the 360 kW PV array's peak yield power for a 2-level inverter offered by IGBT manufacturer Semikron. The particular Semisel online application is used, having the RMS output voltage, yield power, efficiency, exchanging recurrence and overload factor as inputs.

For the maximal power of 360 kW and a worst-case effectiveness of 85%, the RMS current through inverter is equivalent to 611.3 A:

$$I_{INV\_RMS} = \frac{P_{INV}}{3.V_{PHASE}} X \frac{100}{85} = 6.11.3A \quad 5)$$

Sizing the PWM coils inductance is done considering a 5% ripple current from the peak value of the injected current, which is:

$$I_{INV\_PEAK} = I_{INV\_RMS} x\sqrt{2} = 864.5A \quad 6)$$

Hence, the peak-to-peak value of current ripple is:

$$I_{INV\_PEAK} = 0.05\ X\ I_{INV\_PEAK} = 43.2A \quad 7)$$

The PWM coils inductance is calculated with [4]:

$$L_{PWM} = (\sqrt{3}.V_{DC})/(12.\delta.f_{COM}.I_{RIPPLE\_PEAK}) = 0.62mH \quad 8)$$

δ =the overload factor;

f_{COM} =the switching frequency of the inverter.

The value of the DC-interface capacitor is registered to limit the DC-connected voltage ripple to 5% of the DC-Link voltage. For a sinusoidal waveform, the normal estimate of the current

*Iavg*is 63.6% from the peak value or 0.9 from the RMS esteem:

$$I_{AVG} = 0.9 \,.\, I_{INV\_RMS} = 0.9X611=550.18A \qquad 9)$$

The peak-to-peak ripple value of the DC-Link voltage is imposed to 5%:

$$V_{RIPPLE\_PEAK} = 0.05 \cdot V_{DC\_LINK}=0.05 \cdot 700=35V \qquad 10)$$

The capacitor's value *CDC-LINK* can now be determined with

$$C_{DC\_LINK} \geq \frac{I_{INV\_AVG}}{2 \cdot \omega \cdot V_{RIPPLE\_PEAK}} \geq \frac{550{,}18}{2 \cdot 314 \cdot 35} \geq 25018 \mu f \qquad 11)$$

where: ω= the angular frequency corresponding to the 50Hz grid.

The rated voltage *VRATED_CDC* is recommended to be at least20 % higher than the operating voltage:

$$V_{RATED\_CDC} \geq 120\% \cdot V_{DC\_LINK} \geq 840 \qquad 12)$$

Considering (11) and (12), few capacitors must be arranged in parallel to achieve the expansive capacitance needed at this high voltage esteem. The chosen IGBT switching transistors of the inverter are SKiiP3614GB12E46DUW, liquid cooled.

The specialized Semisel online application was utilized. Considering the boost converter's curl resistance of 35 MΩ and the IGBT and diode misfortunes, the efficiency $\eta$of the converter is evaluated to be 90%. The duty cycle *Dmax*at the small input voltage *Vmin*can be figured with [4]:

$$M_{MAX} = 1 - \frac{V_{MIN} \cdot \eta}{V_{DC\_LINK}}=0.61 \qquad 13)$$

The maximal current through the IGBT can be computed with [4]:

$$I_{IGBT\_MAX}=2 \cdot I_{OUT\_RMS} \cdot (D_{MAX} + 1) = 1973.6A \qquad 14)$$

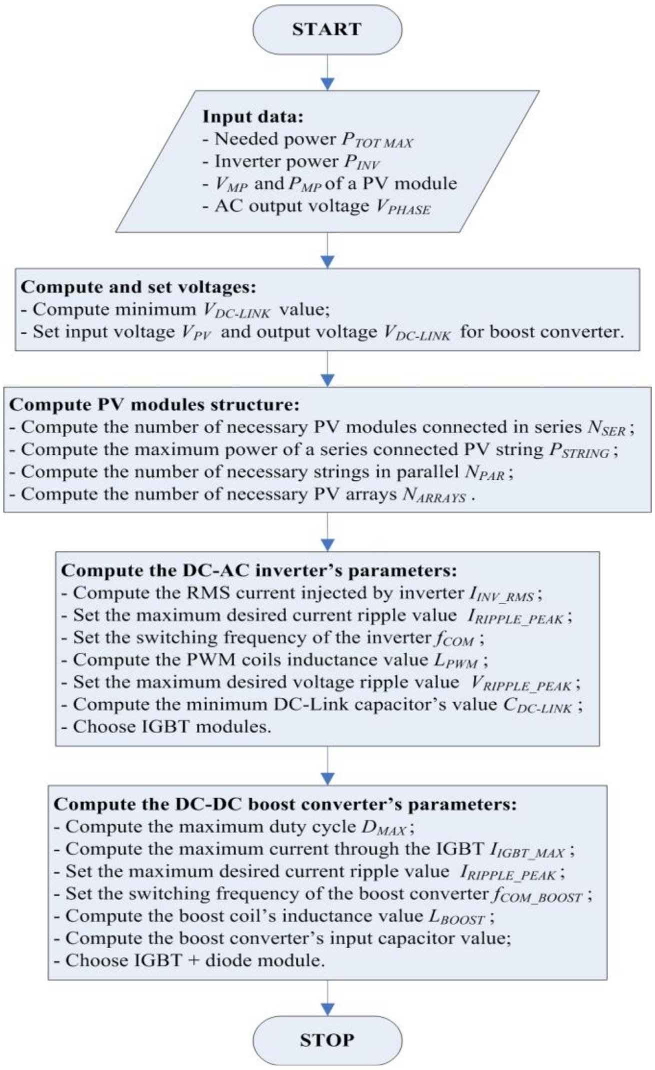

measuring the L_{BOOST} coil inductance is done considering a 5%swell current from the extreme current through the IGBT. Hence, the top-to-peak value of current swell is

$$I_{RIPPLE\_PEAK} = 0.05 \cdot I_{IGBT_{MAX}} = 98.6A \qquad 15)$$

The minimum LBOOST coil inductance is calculated with [5]:

$$I_{BOOST} \geq \frac{V_{MIN} \cdot (V_{DC_{LINK}} - V_{MIN})}{I_{RIPPLE\_PEAK} \cdot f_{COM\_BOOST} \cdot V_{DC\_LINK}} \qquad 16)$$

III. SIMULATION OF ONE 360 KW PHOTOVOLTAIC ARRAY GENERATOR

By utilizing the designing parameters of the PV exhibited beneath and the information from datasheet, a simulation of a field with PV cells corresponding to one of the 28 inverters was done in the Simulink module which has a place with MATLAB.

The Simulink model of the PV field is worked by using elements from the library SimPower Systems. The understanding method is of discrete type and uses a fix venture of 1 зs. The control system framework operates at a testing venture of 100 зs, in order to reproduce as accurate as possible the advanced control and respectively to be appropriate for stacking in microcontrollers and in creating stage as dSPACE.

The model of PV framework includes the configuration of the number of PV cells assemble , as well as the possibility to access different predefined models of panels from several companies. The Sanyo HIP225HDE1 model was selected.

The field with PV cells, The DC-DC converter, three-phase inverter, with the dedicated control system MMPT;

The control system MPPT allows for a maximum energy recovering, regardless to temperature and light. The voltage VPV and the current IPV are continuously measured to conclude power removed from the board

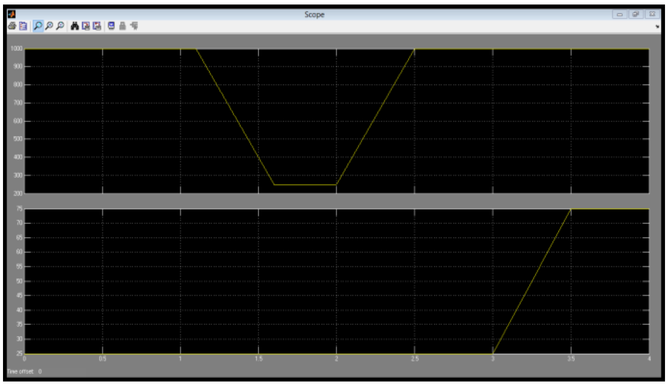

Fig. 4. The evolution of the solar irradiance (top) and PV cell temperature (bottom) during simulation.

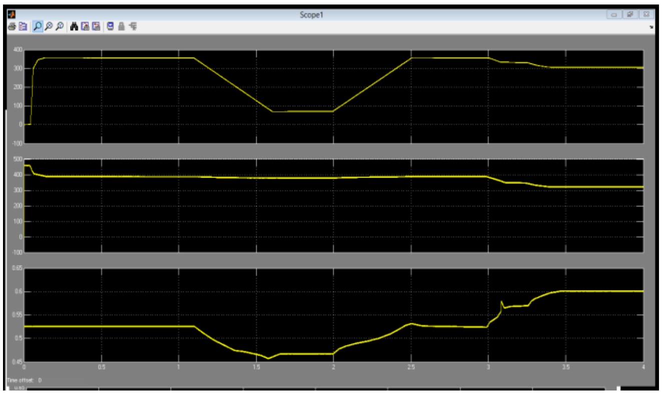

Fig. 5. The waveforms at the boost converter side during simulation: the output power (top), the input voltage (middle) and the duty cycle (bottom).

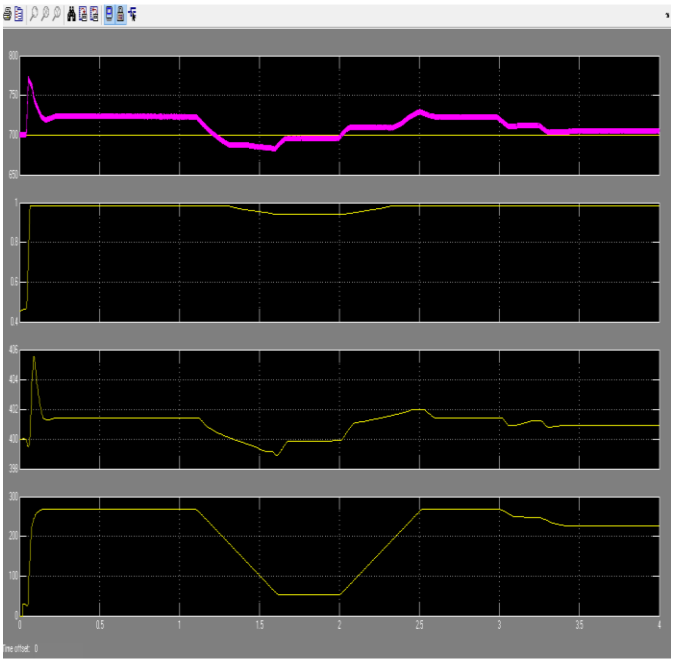

Fig. 6. The waveforms at the inverter side during simulation. From top to bottom: the reference and measured DC-Link voltage, the duty cycle, the RMS line voltage, the RMS phase current.

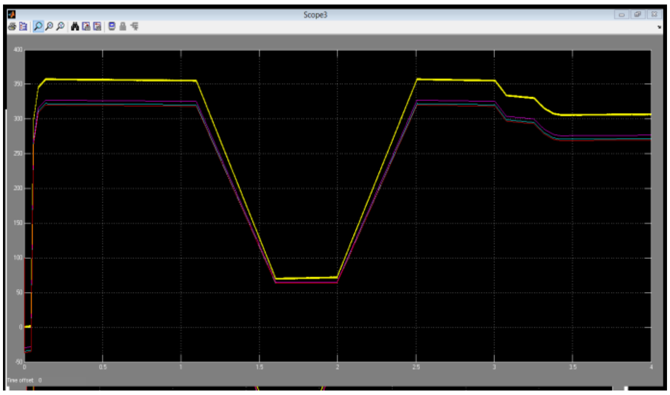

Fig. 7. The evolution of the active powers during simulation, from the PV array to the MV grid.

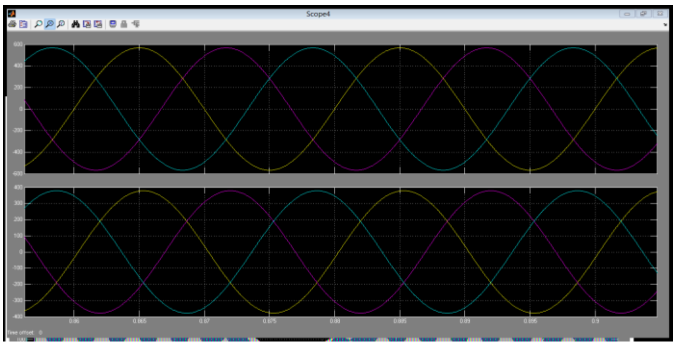

Fig. 8. Detail of the waveforms of the phase voltages (top) and currents (bottom) at the output of the inverter.

The productivity of the power transformation depends enormously on the lift and coupling inductors. An effectiveness of 0.88 is acquired for the boost converter and an proficiency of 0.94 is obtained for the inverter.

In order to estimate the symphonious twisting level for the voltage in the 0.4 kV bars, as well as the additional current injected into the system, a special analysis tool was utilized (FFT Analysis Tool) from the client graphic interface "PowerGUI".By using this instrument one can see the proficiency of the coil used for coupling to the system with the exchanging frequency 2.5 kHz and little values for the harmonic distortion of voltage (2.3%) and separately for current (0.8%). In the 20 kV the total aggregate consonant is even smaller (< 1%) because of the transformer's inductance.

IV. CONCLUSIONS

The simulation of the planned PV park by utilizing Simulink made possible the testing and objective of its stability and effectiveness. The PV generation network behaves well in various conditions of solar light and temperature of PV panels, saving its stability and succeeding in extracting the most power from the PV panels attributable to the control algorithm MPPT.

The PV age system is additionally providing a voltage portrayed by a very good quality: the total symphonious contortion in the 0.4 kV panels has a low value (2.3%) and in the 20 kV bars the distortion is much little (< 1%). These conclusions can be deduced based on the view of got data and waveforms. We can presume that the PV generating framework was designed appropriately.

REFERENCES:

[1] J. M. Carrasco, L. G. Franquelo, J. T. Bialasiewicz, E. Galvan, R. C. P. Guisado, Ma. A. M. Prats, J. I. Leon, N. Moreno-Alfonso, "Power Electronic Systems for the Grid Integration of Renewable Energy Sources: A Survey", IEEE Trans. on Ind. Electr., Vol. 53, Issue 4, June 2006, pp. 1002 – 1016.

[2] M, A. Green, K. Emery, Y. Hishikawa and W. Warta,, Solar cell efficiency tables (version 37)." Progress in Photovoltaics: Research and Applications, vol. 19, pp. 84-92 (2011)

[3] J. Simon and G. Mosey, "Feasibility Study of Economics and Performance of Solar Photovoltaics at the Sky Park Landfill Site in Eau Claire, Wisconsin", National Renewable Energy Laboratory, available at http://www.nrel.gov/docs/fy13osti/56995.pdf (2013)

[4] G. K. Kasal and B. Singh, "Voltage and Frequency Controllers for an Asynchronous Generator-Based Isolated Wind Energy Conversion System", IEEE Trans. on Energy Conv., Vol. 26, Issue 2, pp. 402-416, 2011

[5] Brigitte Hauke, "Basic Calculation of a Boost Converter's Power Stage", Texas Instruments Application Report SLVA372C, 2014.

6) W. Hongbin, T. Xiaofeng, "Three phase photovoltaic grid-connected generation technology with MPPT function and voltage control", Int. Conf. on Power Electr. and Drive Systems (PEDS 2009), pp. 1295-1300, 2-5 Nov. 2009.

7) M.I. Hossain, S.A. Khan, M. Shafiullah, M.J. Hossain, "Design and implementation of MPPT controlled grid connected photovoltaic system", 2011 IEEE Symposium on Computers & Informatics (ISCI), pp. 284-289, 20-23 March 2011.

8) R.-L. Lin, C. Hong-Zhi, "MPPT photovoltaic wide load-range ZVS phase-shift full-bridge charger with DClink current regulation", 2012 IEEE Industry Applications Society Annual Meeting (IAS), pp.1-8, 7-11 Oct. 2012.

9) M. A. G. de Brito, L. P. Sampaio, G. Luigi, G. A. e Melo and C. A. Canesin, "Comparative analysis of MPPT techniques for PV applications", 2011 Int. Conf. on Clean Electrical Power (ICCEP), Ischia, pp. 99-104, 2011.

10) H. Guan-Chyun, C. Hung-Liang, C. Yaohwa, T. Chee-Ming, S. Shian

11) Brigitte Hauke, "Basic Calculation of a Boost Converter's Power Stage", Texas Instruments Application Report SLVA372C, 2014.

12) Robert W. Erickson, DC–DC Power Converters, Wiley Encyclopedia of Electrical and Electronics Engineering, 2007

13) J. Arai, T. Takada, K. Koyanagi and R. Yokoyama, "Power Smoothing by Controlling Stored Energy in Capacitor of Photovoltaic Power System", Power and Energy Engineering Conference (APPEEC), 2012 Asia-Pacific, Shanghai, 2012, pp. 1-5.

14) M, A. Green, K. Emery, Y. Hishikawa and W. Warta,, Solar cell efficiency tables (version 37)." Progress in Photovoltaics: Research and Applications, vol. 19, pp. 84-92 (2011).